Isolation of Cellulose Nanofibers from Para Rubberwood and Their Reinforcing Effect in Poly(vinyl alcohol) Composites

Walailuck Kamphunthong,[1] Peter Hornsby,[2] Kalyanee Sirisinha[1]

[1]*Department of Chemistry, Faculty of Science, Mahidol University, Bangkok 10400, Thailand*
[2]*Polymers Cluster, School of Mechanical and Aerospace Engineering, Queen's University Belfast, Belfast BT9 5AH, United Kingdom*

Received 16 June 2011; accepted 18 September 2011
DOI 10.1002/app.35642
Published online 16 January 2012 in Wiley Online Library (wileyonlinelibrary.com).

ABSTRACT: In this article, we present an efficient method for isolating cellulose nanofibers from para rubberwood sawdust with a combination of chemical, mechanical, and ultrasonic treatments. The effects of the alkali concentration and treatment pathway on the cellulose structure and properties are discussed. The reinforcing efficiency of the resulting fibers on poly(vinyl alcohol) (PVA) composites was characterized. Field emission scanning electron microscopy and atomic force microscopy results revealed a well-organized network of the nanofibers with diameters in the range 20–80 nm and lengths of micrometer-scale dimensions. Fibers with a high crystallinity of 83% having a cellulose I structure were prepared by an isolation process involving a mild alkali solution and delignification before acid hydrolysis. Clear composite films with significant improvements in their modulus (by 100%) and strength (by 80%) were obtained by the addition of 7 wt % fiber. Strong interaction between the fibers and PVA was evident from dynamic mechanical analysis and differential scanning calorimetry. © 2012 Wiley Periodicals, Inc. J Appl Polym Sci 125: 1642–1651, 2012

Key words: biopolymers; nanocomposites; nanofiber

INTRODUCTION

The para rubber tree (*Hevea brasiliensis*) is an economically important crop grown in Thailand. Rubber latex is collected and used as a primary source for the glove and tire industries. Para rubberwood is used mainly in the production of furniture, and a large amount of sawdust is produced as industrial waste. Wood fibers generally have a high elastic modulus of about 10 GPa.[1] However, by the extraction of wood and other cellulosic feedstocks with an appropriate isolation method, crystalline cellulose or cellulose nanofibers with a modulus comparable to commercial E-glass fiber (~ 100 GPa) can be obtained.[2,3] These cellulose nanofibers have great potential for use as reinforcements in biocomposites for construction, automotives, and furniture because of their high strength, recyclability, and environmental sustainability.[4] To date, much research has focused on the isolation of cellulose nanofibers from nonwood resources, for example, cotton,[5] flax,[6,7] and wheat straw.[8–10] Relatively few publications have been written on the isolation of cellulose nanofibers from wood sources. This is partly due to the higher amount of lignin (~ 20 wt %) in wood compared to nonwood materials (2–3 wt % lignin), which has to be removed from the fibers.

In the case of nonwood feedstocks, chemical treatment, such as acid hydrolysis, or mechanical processing, for example, grinding or cryocrushing, are normally used in the extraction of cellulose nanofibers. The fibers obtained may vary in their structure and properties. The use of strong chemicals, such as chlorine dioxide (ClO_2) applied in the bleaching process, reduces the chain length of cellulose significantly and limits the reinforcing ability of the fibers.[11] The transformation of the cellulose structure from native cellulose I into cellulose II is possible after alkali treatment (mercerization).[12] Generally, cellulose displays six different polymorphs, namely, I, II, III_I, III_{II}, IV_I, and IV_{II}, with the possibility of conversion from one to another. Normally, it is the cellulose I form that has the highest strength.[12,13]

In comparison to nonwood resources, the isolation of cellulose nanofibers from wood requires a more complicated and multistep procedure. Chen et al.[14] attempted to produce cellulose nanofibers from wood powder with high-intensity ultrasonication combined with chemical treatment with acidified sodium chlorite ($NaClO_2$) and potassium hydroxide. The delignification step was repeated several times to obtain a white product. Abe et al.[15] introduced a

Correspondence to: K. Sirisinha (sckpr@mahidol.ac.th).
Contract grant sponsor: Thailand Research Fund through the Royal Golden Jubilee Ph. D. Program; contract grant number: PHD 0174/2549.

method to obtain cellulose nanofibers with a uniform width of 15 nm from pine wood. In this approach, a slurry of 1 wt % purified cellulose was passed through a ball mill at 1500 rpm to produce a very fine network of cellulose nanofibers. Bledzki and Gassan[1] calculated the elastic modulus of cellulose chains, reporting values of up to 250 GPa, and stated that the nanofibers from soft wood exhibited a higher Young's modulus compared to those from nonwood sources, such as cotton, flax, and hemp.

Current research on cellulose nanofiber–polymer composites has been extensively reviewed.[16–20] The two major fabrication techniques most commonly considered for the production of cellulose nanocomposites are solution casting[20,21] and melt blending.[22,23] For conventional melt-processing methods, such as compression molding or extrusion, freeze-dried cellulose has been used. However, there are significant problems associated with the feeding and dispersion of nanofibers into the polymer melt; these result in agglomeration and/or orientation of the nanofibers during processing.[24] In contrast, poly(vinyl alcohol) (PVA) and other water-soluble polymers are more suited for solution blending with cellulose nanofiber suspensions. Several reports have focused on PVA composites reinforced with cellulose whiskers or cellulose nanocrystals,[19,20,25] which occur as rodlike particles. For example, Roohani et al.[20] prepared cotton nanowhisker-reinforced PVA nanocomposite films. The degree of hydrolysis of the PVA was varied to investigate the effect of interaction between the whisker and the matrix on properties of the composites.[20] Kvien and Oksman[26] studied the orientation of cellulose whiskers in PVA and the dynamic mechanical properties of composite products.

In this work, we used para rubberwood sawdust as an alternative feedstock to produce cellulose nanofibers, with a view to obtaining cellulose nanofibers with a high crystallinity and thermal stability with a combination of chemical, mechanical, and ultrasonic treatments. Emphasis was given to the characterization of the structure and properties of the cellulose nanofibers produced by these means and their reinforcing efficiency in PVA composites, made by a solution casting technique and tested under static and dynamic conditions, together with the thermal and structural characteristics of these materials. A subsequent article will report the means for the preparation of para rubberwood nanofiber–polymer composites by melt processing.

EXPERIMENTAL

Materials

Para rubber sawdust was obtained from P. Kitsiri Co., Ltd. (Pathum Thani, Thailand). Cellulose nanofibers were extracted from this feedstock with sodium hydroxide (NaOH), sodium acetate trihydrate ($C_2H_3NaO_2 \cdot 3H_2O$), sulfuric acid (H_2SO_4) from Lab Scan Analytical Science Co., Ltd. (Samutsakorn, Thailand), and $NaClO_2$ from Ajax Finechem Pty, Ltd. (Sydney, Australia). PVA (P2C20), supplied by PVAXX, Ltd. (London, United Kingdom), was used as the polymer matrix.

Isolation of cellulose nanofibers from para rubberwood

The extraction of nanofibers from para rubber sawdust required multiple steps. First, the sawdust was passed through a 70-mesh stainless steel sieve and then dried overnight at 65°C before pretreatment with an alkali solution. We did this by soaking the sawdust in NaOH solution at room temperature for 2 h followed by washing it several times with distilled water. The pretreated fibers were delignified with an $NaClO_2$ solution with a pulp-to-liquor ratio of 1 : 1 in 0.1*M* sodium acetate buffer (pH 4.9) for 2 h at 70°C and then washed with distilled water. The white delignified product was then hydrolyzed with 64 wt % sulfuric acid for 1 h at 45°C with stirring and was rinsed several times with distilled water. The insoluble portion remaining was collected and dried at room temperature. The chemically treated fibers were cryogenically crushed with a pestle and mortar and then soaked in distilled water to prepare a suspension. This was dispersed in a T80 Ultra-TURRAX homogenizer (Staufen, Germany) with a power of 230 VAC and speed of 15,000 rpm for 1 h. The homogenized fibers were then defibrillated with ultrasound for 10 min in an ice bath. After this stage, a stable, translucent aqueous suspension of cellulose nanofibers was formed, which did not sediment or flocculate. These were subsequently used in the preparation of the PVA composites. For scanning electron microscopy (SEM) and atomic force microscopy (AFM) characterization, dried nanofibers were produced by freeze drying.

Preparation of the PVA nanocomposites

Composite films of PVA and cellulose nanofibers were prepared by solution casting to yield an approximate thickness of 200 μm. To this end, PVA powder was first dissolved in distilled water and stirred at 90°C for 1 h to produce a 10 wt % PVA solution. The cellulose suspension was subsequently mixed with the PVA solution at ambient temperature for 30 min to produce mixtures with increasing nanofiber loadings. Each mixture was then cast onto a Petri dish and left standing at ambient temperature until the water had evaporated and the sample weight was constant. The samples were then dried

at 40°C overnight to avoid the plasticizing effect of moisture during characterization.[6]

Characterization and testing

The morphology of the sawdust feedstock and the cellulose nanofibers was investigated with a JEOL JSM-6500F field emission scanning electron microscope (Herts, United Kingdom) with a resolution of 5 nm at 2 kV. Freeze-dried cellulose, obtained from a suspension containing 5 wt % cellulose, was held on a sample holder with adhesive tape and then sputter-coated with gold to prevent the buildup of an electrostatic charge. The morphology of cellulose nanofibers was also analyzed with a Nano Scope IIIa model NS3a multimode atomic force microscope (Plainview, NY) in the tapping mode. Samples of freeze-dried cellulose were deposited onto an aluminum sample holder and then scanned with a silicon tip with a radius of 10 nm over a scan size of 1 μm.

The crystal structure and crystallinity of the cellulose nanofibers were examined with a Bruker D8 Advance X-ray diffractometer (Madison, WI) with a generator voltage of 40 kV and a current of 40 mA. The samples were scanned at a speed of 5 s per step over a 2θ range from 10 to 30°. From the X-ray diffraction (XRD) diffraction pattern, the amorphous contribution in the cellulose was determined and subtracted. The degree of mercerization (C_{IIr}) and the crystallinity index (I_c) were calculated with eqs. (1)[27] and (2):[16,28]

$$C_{IIr} = \frac{I_{r12.1}}{I_{r12.1} + 0.5(I_{r14.1} + I_{16.1})} \times 100 \quad (1)$$

where I_r is the relative intensity reading at each specific diffraction peak with respect to the intensity reading at a maximum peak in the XRD pattern:

$$I_C = \frac{I_{(002)} - I_{(am)} \times 100}{I_{(002)}} \quad (2)$$

where $I_{(002)}$ is the peak intensity at 2θ equal to 22.7° and attributed to a specific characteristic of crystalline cellulose[16,28] and $I_{(am)}$ is the intensity at 2θ equal to 18°, corresponding to the amorphous portion of the cellulosic material.

The decomposition behavior of para rubber sawdust and cellulose nanofibers was evaluated using a PerkinElmer TGA7 (Schwerzenbach, Switzerland) in an oxygen atmosphere, using a flow rate of 60 mL of/min. The samples were heated from 100 to 650°C at a rate of 10°C/min.

Fourier transform infrared (FTIR) spectra were obtained with an Equinox 55 FTIR spectrometer (Madison, WI) in the transmission mode. The samples were ground and mixed with KBr before scanning over wave numbers of 4000–600 cm^{-1}. The chemical structures of the rubber sawdust before and after treatment were compared. For this purpose, the spectra obtained were normalized against the CH_2 stretching vibrations at 2900 cm^{-1}.

Tensile testing was carried out with a model 4411 Instron universal tensiometer (Canton, MA). Dumbbell-shaped specimens ($3 \times 62.5 \times 1$ mm^3) were tested at 23°C with a crosshead speed of 50 mm/min with a 5-kN load cell. The samples were conditioned at 40°C and 50% humidity before testing.

The dynamic mechanical behavior of the composites was investigated with a Triton DMA 2000 dynamic mechanical analyzer (Suarlee, Belgium) in the tensile mode. The specimen was cut into a rectangular bar with a size of $10 \times 40 \times 0.3$ mm^3. The samples were heated from 30 to 120°C at a rate of 5°C/min. The test was performed at a frequency of 1 Hz and a strain amplitude of 0.1%.

The crystallization and melting behavior of the PVA nanocomposites were monitored with a PerkinElmer DSC 6 modular thermal analyzer (Boston, MA). Approximately 5–7 mg of the samples was heated from 20 to 230°C at a scanning rate of 10°C/min in a nitrogen environment and then held at 230°C for 1 min. The samples were then cooled to 20°C at the same rate. The melting temperature (T_m) and crystallization temperatures (T_c's) were then recorded. The normalized heat of fusion was determined from the relationship between the heat of fusion and the weight fraction of the polymer in the composites, whereas the percentage crystallinity (X_c) was calculated from the ratio of the normalized heat of fusion of the composites with respect to 100% crystalline PVA, taken as 161.6 J/g.[20]

RESULTS AND DISCUSSION

Characterization of the cellulose nanofibers

Figure 1(a) shows an electron micrograph of the para rubber feedstock showing the variation in the sawdust particle size, with some particles being larger than 1 mm. After the isolation process, a well-organized network of cellulose nanofibers was obtained [Fig. 1(b)]. Also, Figure 1(c) reveals the morphology of the cellulose nanofibers under high magnification by field emission scanning electron microscopy (FE-SEM). The individual nature of the cellulose nanofibers could be clearly seen, and they formed a very fine network structure. The diameters of the nanofibers were analyzed with an Olympus image analysis program (Olympus, Tokyo, Japan) on basis of the measurement of approximately 500 fibers seen in the FE-SEM images (Fig. 2). The majority of the fibers had diameters in the range 20–80 nm, with lengths on the order of micrometers. The

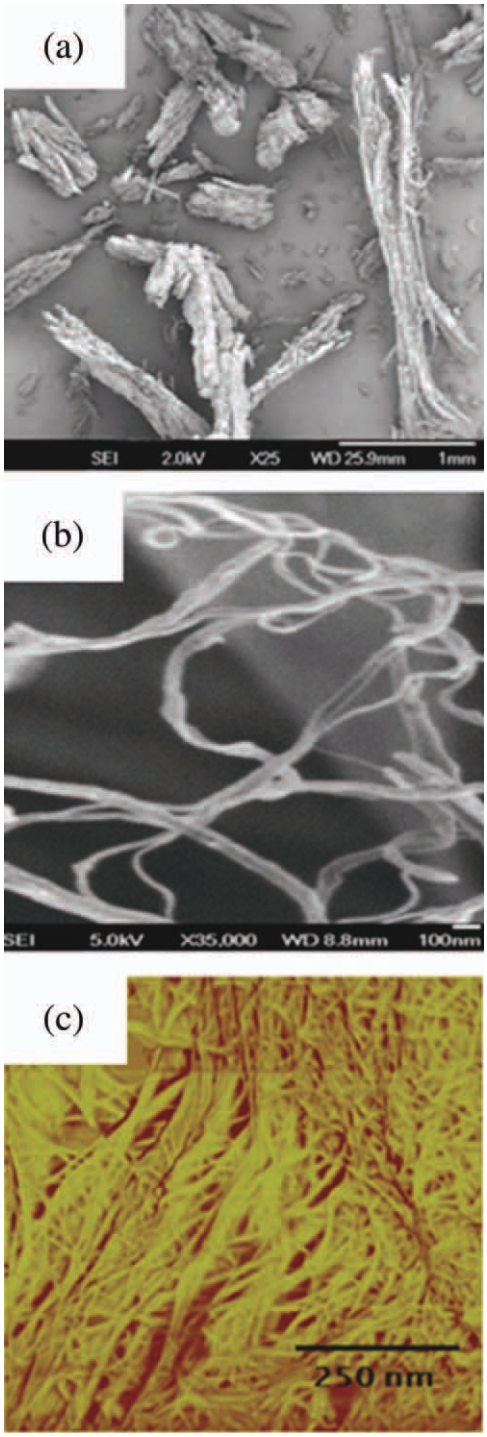

Figure 1 (a) SEM image of para rubber sawdust, (b) AFM image of freeze-dried cellulose nanofibers analyzed in the tapping mode, and (c) FE-SEM image of freeze-dried cellulose nanofibers. [Color figure can be viewed in the online issue, which is available at wileyonlinelibrary.com.]

size of the nanofibers from para rubberwood was similar to the size of the nanofibers reported from flax, cotton, soy hulls, and wheat straw, which typically have diameters in the range 20–90 nm.[6,8,20] In the case of soybean nanofibers, the range of fiber widths was between 50 and 100 nm.[5] However, it

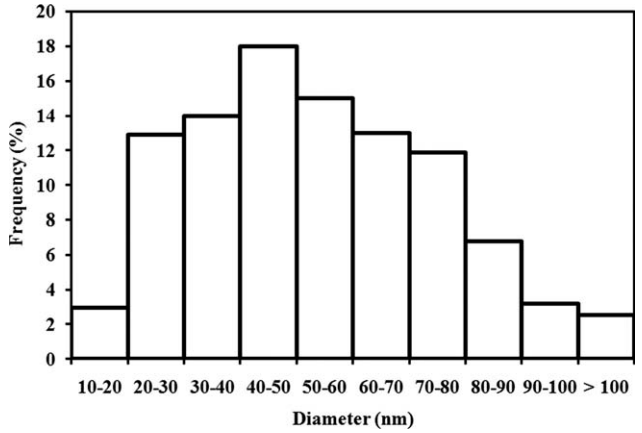

Figure 2 Size distribution of freeze-dried cellulose nanofibers analyzed from FE-SEM images.

was difficult to identify an exact length of the nanofibers prepared in this investigation. However, it was evident that their lengths were greater than 1000 nm, which is generally longer than those of typical nanowhiskers, between 100 and 300 nm; this suggested that their higher aspect ratio would give a greater reinforcing efficiency.

Figure 3 shows XRD patterns for the para rubber sawdust before and after treatment. The neat sawdust showed peaks characteristic of a native cellulose I structure at $2\theta = 22.7^\circ$ and two overlapping peaks at 14 and 16°.[16,25] After alkali treatment with an NaOH solution at a concentration of 17.5 wt %, the polymorphic transformation of cellulose I into cellulose II was observed. The main XRD peak shifted from 2θ at 22.7–22°. The degree of mercerization was calculated to be 15% in this case. The transformation of the cellulose structure has been found previously, as in the case of pine wood sawdust.[12] The ability of cellulose I to transform into cellulose II depends not only on the alkali concentration but also on the time of treatment

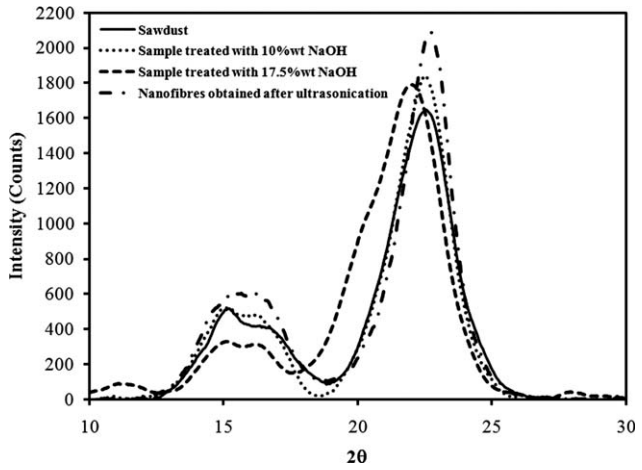

Figure 3 XRD patterns for the para rubber sawdust and its treated samples.

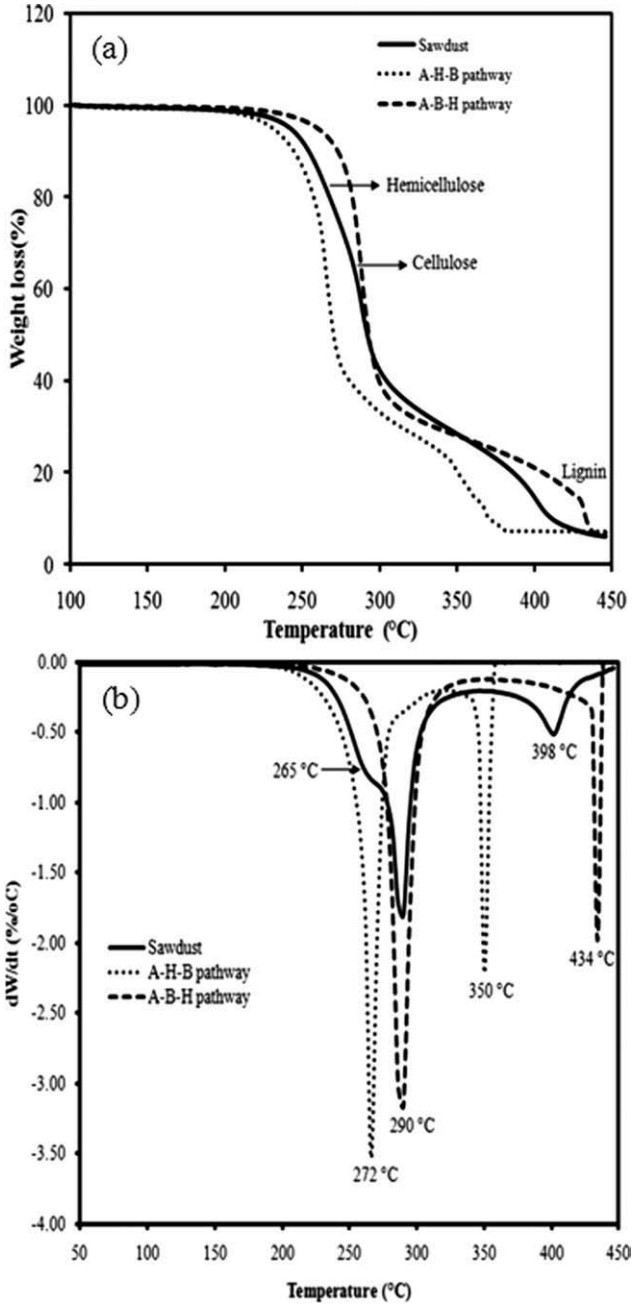

Figure 4 (a) TGA and (b) its derivative thermograms of neat sawdust and samples prepared with different treatment procedures. The test was performed under an O_2 atmosphere with a heating rate of 10°/min.

and the composition of the feedstock.[12] To prevent the transformation of the cellulose structure, the concentration of NaOH solution was reduced from 17.5 wt %, which is a common concentration used in alkali treatment,[6,8] to 10.0 wt %. As a result, no crystal conversion of cellulose I into cellulose II was seen. Hence, the XRD patterns of the fibers obtained after alkali treatment with 10 wt % NaOH and after ultrasonication were similar to those of the native sawdust, which had a cellulose I structure. This indicated that the structure of cellulose could be maintained during defibrillation of the fibers.

Figure 4 shows TGA thermograms of the neat wood sawdust and the nanofibers prepared with different treatment pathways. The A–H–B pathway began with alkali treatment (A), followed by acid hydrolysis (H) and then bleaching (B) to enable delignification. For the A–B–H pathway, bleaching was performed before hydrolysis. The thermal stability of the fibers obtained from both pathways was compared. The onset temperature of decomposition ($T_{d\ \mathrm{onset}}$), determined from the temperature at 10% weight loss, and the decomposition temperature (T_d) of various samples are summarized in Table I. It can be seen from Figure 4(a,b) and Table I that the neat sawdust had a $T_{d\ \mathrm{onset}}$ of approximately 250°C with three decomposition transitions. The principal transition, attributed to the decomposition of the cellulosic component occurred at 290°C. An initial transition, at approximately 265°C, corresponded to the decomposition of hemicellulose. A terminal event around 440°C was attributed to the decomposition of lignin, which had a more thermally stable aromatic structure.[29] After chemical treatment, the transition at 265°C disappeared; this indicated that complete elimination of hemicellulose occurred. However, the transition at high temperature, which is a characteristic of lignin, was still present; this implied that there was some residual lignin left in the samples. The incomplete removal of lignin with normal oxidizing agents was previously been reported for wheat straw, which contained a similar content of lignin (ca. 20 wt %) as the sawdust used in this study.[8] However, the presence of residual lignin was reported to have a positive effect on the thermal stability and strength of the fibers obtained.[30]

In this study, the use of a strong alkali solution (17.5 wt % NaOH) resulted in a fiber with a lower

TABLE I
Properties of the Neat Sawdust and Its Treated Samples

Sample	$T_{d\ \mathrm{onset}}$ °C	T_d °C	Crystallinity index[a] %
Neat sawdust	254	290	57.86
Sample after treatment with 10 wt % NaOH	274	290	66.61
Sample after treatment with 17.5 wt % NaOH	230	270	68.64
Sample after treatment with the A–H–B pathway	246	272	N/A
Sample after treatment with the A–B–H pathway	274	290	N/A
Cellulose nanofibers after chemical and ultrasonic treatment	274	290	83.14

N/A, not applicable.
[a] Calculated from XRD results with eq. (2).

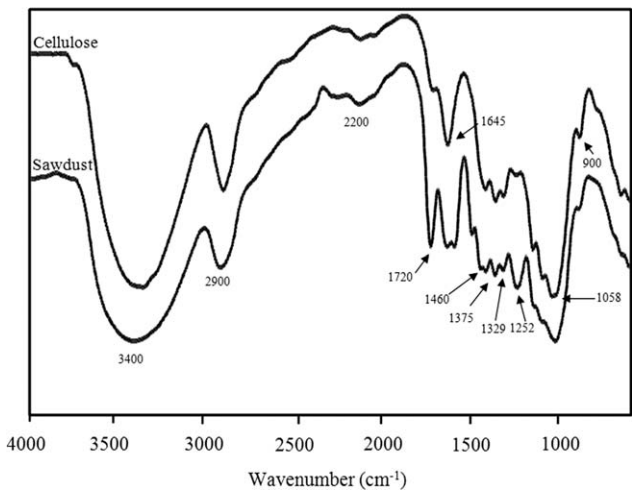

Figure 5 FTIR spectra of the untreated rubber sawdust and freeze-dried cellulose nanofibers obtained after chemical and ultrasonic treatments.

$T_{d\ \text{onset}}$ of 230°C and a T_d of 270°C (Table I); this reflected the adverse effect of the alkali solution on the thermal stability of the fibers. The fibers that were treated with the A–B–H pathway showed a 20°C higher $T_{d\ \text{onset}}$ and T_d than those prepared from the A–H–B pathway. A partial destruction of crystalline cellulose may have occurred during delignification of the prehydrolyzed sample with $NaClO_2$. The cellulose nanofibers obtained after ultrasonication exhibited a similar T_d (290°C) with a 20°C higher $T_{d\ \text{onset}}$ (274°C) compared to the untreated sawdust. This demonstrated the suitability of these nanofibers for use in conventional polymer processing, in which the T_m's for thermoplastics frequently exceed 200°C.

Table I also shows the effect of the treatment on the crystallinity index of the various fibers. A systematic increase in crystallinity was observed after the removal of hemicellulose and lignin by chemical treatment and with the application of ultrasound. The final cellulose nanofibers exhibited a crystallinity index of 83%; this was much higher than that of 58% found in the neat sawdust. The increase in crystallinity, together with the removal of lignin and hemicellulose from the fibers, was believed to be the reason for the improved thermal stability of the prepared nanofibers.

Figure 5 shows FTIR spectra of the neat sawdust and the resulting cellulose nanofibers. The main absorptions in the regions of 3400 and 2900 cm^{-1}, corresponding to stretching vibrations of OH and CH_2 groups, respectively, were the principal functional groups found in lignocellulosic materials. The cluster of absorptions at 1460, 1375, 1329, and 1252 cm^{-1} were attributed to the bending of CH, CH_2, and OH, which are typical characteristics of

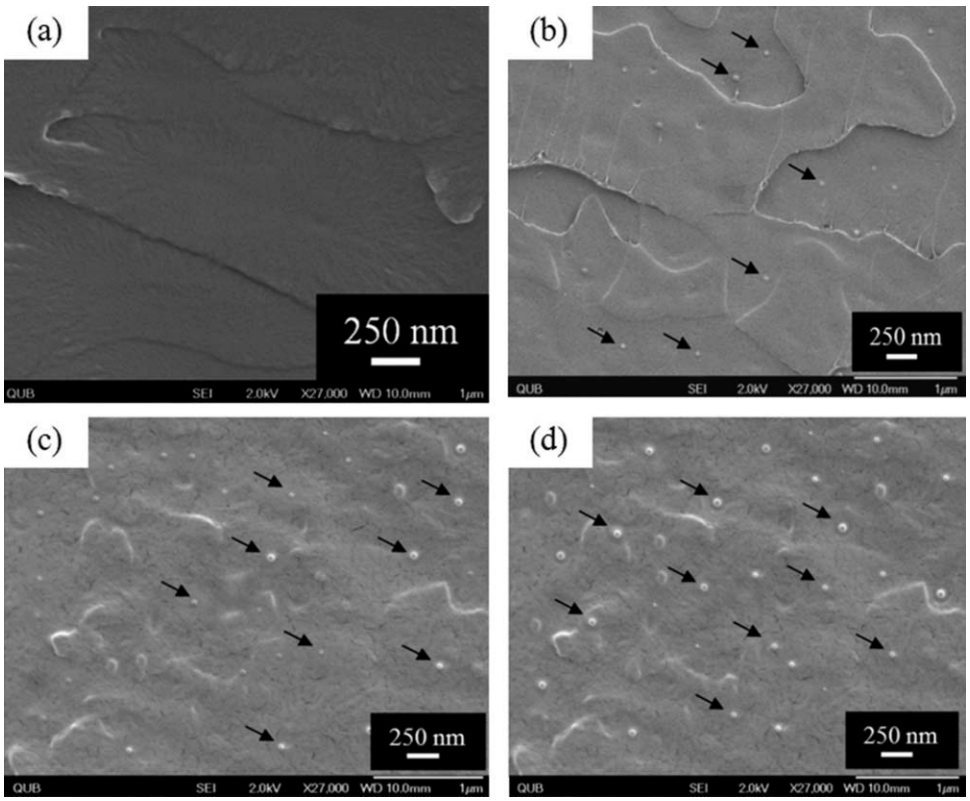

Figure 6 FE-SEM micrograph of the cryogenic fractured surface of (a) PVA and its nanocomposites with (b) 3, (c) 5, and (d) 7 wt % cellulose nanofibers.

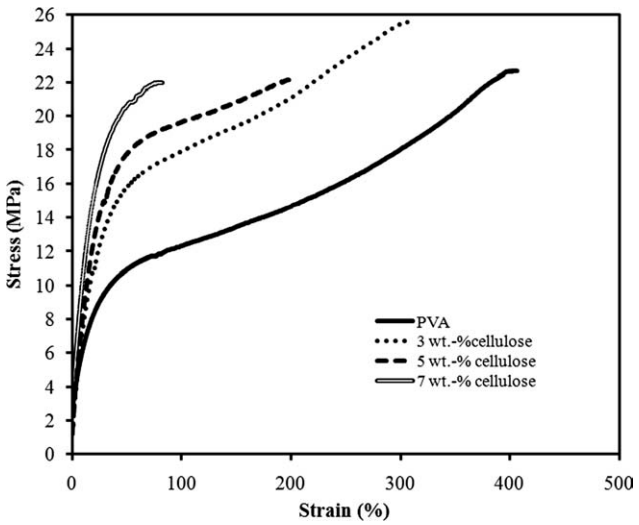

Figure 7 Stress–strain curves of the unmodified PVA and PVA composites filled with cellulose nanofibers. The samples were conditioned at 40°C and 50% humidity before testing at 23°C and 50% humidity.

polysaccharide components. The peak at 1645 cm^{-1} was associated with absorbed water.[8–10] The characteristic peaks of cellulose were evident at 1058 and 900 cm^{-1}, which corresponded to C—O stretching and C—H rocking vibrations.[8] These peaks were prominent in the cellulose nanofiber sample. The sharp peak at 1720 cm^{-1} was attributed to unconjugated carbonyl groups from acetyl moieties found in either hemicelluloses and/or lignin.[8–10] The intensity of this peak was reduced significantly after the isolation process, which indicated a strong reduction of hemicellulose and lignin in the nanocellulose sample. However, a small shoulder at 1720 cm^{-1} existed in the nanofiber sample. This suggest that some residual lignin may have been present in the fibers. The partial removal of lignin in the cellulose nanofibers was confirmed by the reduced intensity of a broad peak around 2200 cm^{-1}, corresponding to the aromatic C=C stretching vibrations of lignin.[8–10] This result of FTIR analysis agreed very well with the TGA results discussed earlier, where the decomposition of residual lignin around 440°C was observed after the treatment process.

PVA/cellulose nanofiber composites

In this study, we prepared PVA nanocomposites by blending a PVA solution with a nanocellulose uspension. The nanofiber was prepared by the pretreatment of para rubber sawdust with a 10 wt % NaOH solution, and then, we performed chemical treatments through the A–B–H pathway. The composite films obtained were transparent for all of the blend compositions. This implied a good dispersion of the fibers without reaggregation during the drying process and also suggested strong interaction between the PVA matrix and the cellulose nanofibers, which inhibited reaggregation of the nanofibers. Figure 6 shows the FE-SEM images of the cryogenic fractured surfaces of pure PVA and its composites. The arrows in the micrographs point to the location of the cellulose nanofibers.

Figure 7 shows the stress–strain curves for the unfilled PVA and PVA biocomposites containing amounts of cellulose nanofibers up to 7 wt %. The effect of the fiber loading on the composite modulus, elongation, and strength are shown in Figure 8. From the stress–strain curves, it was evident that PVA exhibited ductile deformation at room temperature. At low strain (<20%), the stress increased rapidly with increasing strain. Beyond approximately 20% strain, the magnitude of the stress increment with strain decreased until failure occurred at approximately 400% elongation without obvious signs of necking. The incorporation of cellulose nanofibers caused a dramatic increase in the stress at low strain; this reflected the higher modulus of these composites. The stress at break also increased from 22 to 26 MPa when only 3 wt % of the fibers were introduced. More than a 100% improvement in

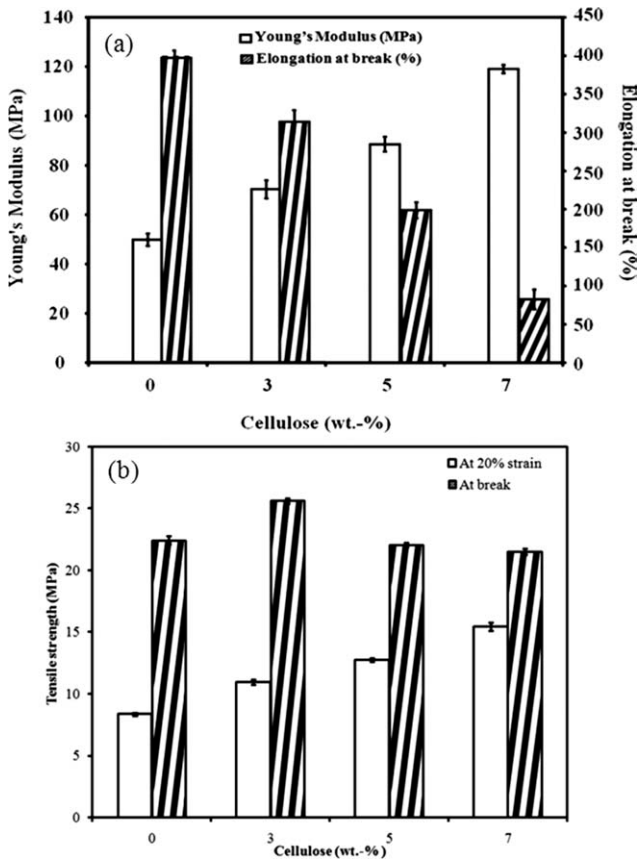

Figure 8 Tensile properties of the PVA/cellulose nanofiber composites: (a) modulus and elongation at break and (b) strength at break and at 20% strain.

TABLE II
Properties of the PVA Composites Filled with Nanocellulose Isolated from Various Cellulosic Feedstocks

Feedstock	Loading (%)	Improvement (%)			Reference
		Stress at yield	Stress at break	Young's modulus	
Para rubber sawdust	3	42	18	40	—
	5	58	0	78	
	7	83	0	138	
Soybean	5	22	N/A	87	11
	10	53	N/A	113	
Microcrystalline cellulose	1	N/A	49	36	7, 10
	3	N/A	45	45	
	5	N/A	−4	73	
Cotton linter	3	19	14	22	20
	6	2	8	25	
	9	24	0	31	

N/A, not applicable.

the modulus and stress at low strain was observed for the composite with only 7 wt % addition of fibers. In contrast, the elongation at break of the composites dropped systematically with increasing fiber loading. However, the composite with 3 wt % fiber still had an elongation of higher than 300%. This indicated that only a small amount of cellulose nanofibers (3 wt %) was needed for a great improvement in the stiffness and strength of PVA. The inherently high strength and modulus of the cellulose nanofibers, combined with a strong bonding between the fibers and the PVA matrix, were considered to be responsible for the significant enhancement in the mechanical properties of these composites. From the literature, it is evident that the reinforcing efficiency of the fibers prepared in this study, in terms of the tensile stress and modulus, was higher than that seen in nanofibers derived from soy beans[11] and cotton linter[20] and was comparable to that found in commercial microcrystalline cellulose.[7,10] Table II summarizes the effects of nanocellulose derived from various kinds of feedstock on the tensile properties of the PVA composites. The data in the table are reported in terms of the percentage of relative property improvement to take account of variations in the properties and testing conditions of the PVA matrix used by different researchers. These results demonstrate the strong potential of cellulose nanofibers extracted from para rubberwood for biocomposite applications.

Figure 9 shows the temperature dependency of the dynamic mechanical behavior of the PVA film and its reinforced para rubberwood nanocellulose composites. The corresponding glass-transition temperatures (T_g), determined from the maximum of the tan δ peak, are listed in Table III. Neat PVA had a T_g of approximately 42°C. The T_g shifted to higher temperatures after fiber addition; this indicated a restriction of polymer chain movements, probably caused by hydrogen bonding between the fibers and the polymer molecules. A drop in the tan δ peak height was also seen after the addition of fibers; this implied that a physical entanglement or network formation was formed inside the composites because of the immobilization of the polymer surrounding the fibers.

It was apparent that there were noticeable differences in the polymer molecular motion at temperatures above and below the T_g of the PVA matrix

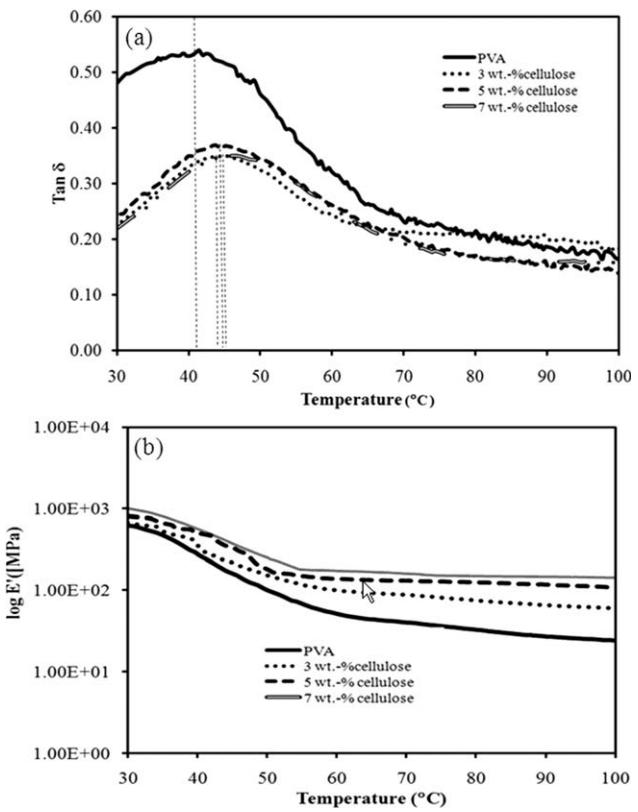

Figure 9 (a) Tan δ and (b) E' as a function of the temperature for various PVA composites filled with cellulose nanofibers. The samples were conditioned at 40°C and 50% humidity before testing.

TABLE III
Dynamic Mechanical Analysis and DSC Results for Various PVA/Cellulose Nanofiber Biocomposites

Cellulose (%)	T_g (°C)	E' (MPa) 30°C	E' (MPa) 70°C	T_m (°C)	ΔH_f (J/g)	Normalized ΔH_f (J/g)[a]	X_c (%)	T_c (°C)	$T_{c\ onset}$ (°C)
0	42	625	40	174	32.3	32.3	20.0	124	142
3	44	673	88	172	21.9	22.6	14.0	112	124
5	45	821	132	169	20.0	21.0	13.0	112	123
7	46	1012	158	169	19.5	21.0	13.0	112	123

[a] The normalized ΔH_f is the heat of fusion of the sample with respect to its weight fraction.

(42°C). A systematic increase in the storage modulus (E') above and below the T_g of PVA was seen clearly with increasing fiber content [Fig. 9(b) and Table III]; this again demonstrated a high reinforcing capacity of the cellulose nanofibers in the PVA matrix. The effect of the fibers was more pronounced beyond the T_g of PVA, where polymer chain movements were less restricted. For example, at 70°C, the composite containing 7 wt % fibers showed an E' of 158 MPa, which was four times higher than that observed for the neat PVA (40 MPa).

Differential scanning calorimetry (DSC) was used to investigate the effect of cellulose nanofibers on the thermal properties of the PVA matrix. Thermal parameters, including the T_m, heat of fusion (ΔH_f), T_c, and onset temperature of crystallization ($T_{c\ onset}$), were analyzed from the DSC thermograms. To eliminate the dilution effect of the PLA matrix, the normalized heat of fusion was determined for the calculation of X_c. The DSC results obtained are given in Table III. PVA exhibited a T_m of 174°C with a crystallinity of 20%. Both T_m and the crystallinity of PVA decreased after the incorporation of cellulose nanofibers. A similar reduction in both properties was also reported by Roohani et al.[20] for cellulose-whisker-reinforced PVA composites. The presence of cellulose nanofibers in the polymer matrix inhibited polymer chain folding, and as a result, less perfect crystals were formed. This could be ascribed to the strong interactions between the fiber and polymer matrix through extensive hydrogen bonding, which limited the capacity of the polymer to form a crystalline domain.[20] The inhibition of polymer crystallization brought about by fiber addition was also evidenced by decreases in T_c and $T_{c\ onset}$. The effects of fiber content on the thermal properties of the composites were not obvious when the fiber content was increased beyond 3 wt %.

CONCLUSIONS

Cellulose nanofibers were prepared from industrial waste derived from para rubberwood and was used as a reinforcing material for PVA to produce biocomposites by solution casting. FE-SEM and AFM images revealed an entangled network of cellulose nanofibers with diameters in the range 20–80 nm and lengths on the order of micrometers. The nanofibers obtained after treatment with a mild alkaline solution (10 wt % NaOH) and the application of ultrasound showed a cellulose I structure that was similar to the native sawdust, with a 20% increase in the crystallinity index. The fibers prepared from the A–B–H pathway (bleaching before hydrolysis) exhibited a better thermal stability than those from the A–H–B pathway. The high reinforcing efficiency of the cellulose nanofibers in PVA was demonstrated through the measurement of the tensile modulus and strength. The Young's modulus and stress at break increased significantly from 49.8 to 70.3 MPa and from 22.4 to 25.6 MPa, respectively, with increasing fiber content from 0 to 3 wt %, whereas the elongation at break dropped slightly from 397 to 314%. These property improvements in the PVA/cellulose nanocomposites could be attributed to strong hydrogen bonding between the cellulose fibers and the PVA matrix. Dynamic mechanical analysis results confirmed this point. The T_g of PVA shifted to higher temperature and E' increased markedly after the addition of the fibers, especially above the T_g of PVA. The presence of fibers also inhibited the polymer crystallization process. The T_m and T_c values and X_c of PVA decreased with nanofiber addition.

The authors are thankful for the technical support provided by the Polymer Processing Research Centre at Queen's University Belfast, in particular by Bronagh Millar, Graham Garrett, and Mark Billham.

References

1. Bledzki, A. K.; Gassan, J. Prog Polym Sci 1999, 24, 221.
2. Sturcova, A.; Davies, G. R.; Eichhorn, S. J. Biomacromolecules 2005, 6, 1055.
3. Hsieh, Y. C.; Yano, H.; Nogi, M.; Eichhorn, S. J. Cellulose 2008, 15, 507.
4. Klemm, D.; Schumann, D.; Kramer, F.; Hebler, N.; Hornung, M.; Schmauder, H. P.; Marsch, S. Adv Polym Sci 2006, 205, 49.
5. Wang, B.; Sain, M. Compos Sci Technol 2007, 67, 2521.
6. Qua, E. H.; Hornsby, P. R.; Sharm, H. S. S.; Lyons, G.; McCal, R. D. J Appl Polym Sci 2009, 113, 2238.

7. Bhatnagar, A.; Sain, M. J. Reinf Plast Compos 2005, 24, 1259.
8. Alemdar, A.; Sain, M. Bioresour Technol 2008, 99, 1664.
9. Sun, X. F.; Sun, R. C.; Su, Y.; Sun, J. X. J Agric Food Chem 2004, 52, 839.
10. Sain, M.; Panthapulakkal, S. Ind Crop Prod 2006, 23, 1.
11. Wang, B.; Sain, M. Compos Sci Technol 2007, 67, 2521.
12. Borysiak, S.; Doczekalska, B. Fibres Text East Eur 2005, 13, 87.
13. Antoinette, O. C. Cellulose 1997, 4, 173.
14. Chen, W.; Yu, H.; Liu, Y.; Chen, P.; Zhang, M.; Hai, Y. Carbohydr Polym 2010, 83, 1804.
15. Abe, K.; Iwamoto, S.; Yano, H. Biomacromolecules 2007, 8, 3276.
16. Teixeiraa, E. D. M.; Pasquinib, D.; Curveloa, A. A. S.; Corradinic, E.; Belgacemd, M. N.; Dufresne, A. Carbohydr Polym 2009, 78, 422.
17. Lee, S. Y.; Mohan, D. J.; Kang, I. A.; Doh, G. H.; Lee, S.; Han, S. O. Fiber Polym 2009, 10, 77.
18. Klemm, D.; Schumann, D.; Kramer, F.; Heßler, N.; Koth, D.; Sultanova, B. Macromol Symp 2010, 280, 60.
19. Nystrm, G.; Mihranyan, A.; Razaq, A.; Lindstrm, T.; Nyholm, L.; Strømme, M. J Phys Chem B 2010, 114, 4178.
20. Roohani, M.; Habibia, Y.; Belgacema, N. M.; Ebrahimb, G.; Karimib, A. N.; Dufresne, A. Eur Polym J 2008, 44, 2489.
21. Nakagaito, A. N.; Fujimura, A.; Sakai, T.; Hama, Y.; Yano, H. Compos Sci Tech 2009, 69, 1293.
22. Jonoobi, M.; Harun, J.; Mathew, A. P.; Oksman, K. Compos Sci Tech 2010, 70, 1742.
23. Oksman, K.; Mathewa, A. P.; Bondesona, D.; Kvien, I. Compos Sci Tech 2006, 66, 2776.
24. Oksman, K.; Mathew, A. P.; Sain, M. Plast Rubber Compos 2009, 38, 396.
25. Azizi Samir, M. A. S.; Alloin, F.; Dufresne, A. Biomacromolecules 2005, 6, 612.
26. Kvien, I.; Oksman, K. Appl Phys A 2007, 87, 641.
27. Mansikkamäkia, P.; Lahtinena, M.; Rissanen, K. Carbohydr Polym 2007, 68, 35.
28. Wang, L.; Zhang, Y.; Gao, P.; Shi, D.; Liu, H.; Gao, H. Biotechnol Bioeng 2006, 93, 443.
29. Ramiah, M. V. J Appl Polym Sci 2003, 14, 1323.
30. Bledzki, A. K.; Sperber, V. E.; Faruk, O. Rapra Rev Rep 2008, 13, 1.